Asian Biomedicine Vol. 6 No. 3 June 2012; 397 - 411 DOI: 10.5372/1905-7415.0603.070

Original article

Altered phosphorylation of mitogen-activated protein kinases in dorsal root ganglia and sciatic nerve of rats with cisplatin-induced neuropathy

Tulaporn Wongtawatchai, Sithiporn Agthong, Athitaya Kaewsema, Vilai Chentanez
Peripheral Nerve Research Unit, Department of Anatomy, Faculty of Medicine, Chulalongkorn University, Bangkok 10330, Thailand

Background: Peripheral neuropathy is a major side effect of cisplatin. Cisplatin preferentially accumulates in the dorsal root ganglia (DRG) and causes neuronal apoptosis. In vitro studies have implicated mitogen-activated protein kinases (MAPKs) in cisplatin-induced apoptosis. However, this has not been confirmed in vivo.
Objective: We studied the phosphorylation of MAPKs, ERK, JNK, and p38, in the DRG and sciatic nerve of rats treated with cisplatin, and correlated it with the neuropathic abnormalities.
Methods: Cisplatin 2 mg/kg was intraperitoneally injected in rats twice a week for five consecutive weeks. Neuropathy was assessed by measuring hind-paw thermal and mechanical thresholds, sciatic motor nerve conduction velocity (MNCV) and morphometric evaluation of DRG and sciatic nerve at various time points after the start of cisplatin treatment. Western blot analysis was done to determine the ratio of phosphorylated to total forms of MAPKs in the DRG and sciatic nerve.
Results: Cisplatin induced transient thermal hypoalgesia, late reduction in MNCV and histopathological abnormalities of DRG and sciatic nerve indicating the neuropathy. ERK was activated in the nerve and DRG in the eighth and twelfth weeks, respectively. Transient activation of JNK in the nerve and DRG was observed only in the first week. At the same time point to JNK, p38 was temporarily inhibited in the DRG. Late activation of ERK was correlated with the presence of pathological changes, suggesting the possible role of ERK in these abnormalities. No correlation between MAPKs and functional abnormalities was observed.
Conclusion: MAPK ERK might play a role in cisplatin-induced structural alterations in the DRG and sciatic nerve and can be the therapeutic target. However, to prove this hypothesis, future studies using the ERK inhibitor must be done.

Keywords: Cisplatin, dorsal root ganglia, MAPK, neuropathy, sciatic nerve

Cisplatin (Cis-diamine-dichloro-platinum) has been used to treat malignancies of various organs, particularly lung, urinary bladder, testis and ovary [1]. It reacts with nuclear DNA by forming intra- and interstrand crosslinks resulting in DNA damages and eventually apoptosis of cancer cells. One of its major side effects is neurotoxicity, characterized by distal symmetrical neuropathy with sensory predominance. Paresthesia, impaired vibration perception, reduced amplitude and velocity of sensory nerve conduction were observed in patients treated with cisplatin [2, 3].

Correspondence to: Dr. Sithiporn Agthong, Department of Anatomy, Faculty of Medicine, Chulalongkorn University, Bangkok 10330, Thailand. E-mail: sagthong@hotmail.com

It has been shown that cisplatin preferentially accumulated in dorsal root ganglia (DRG) when compared to peripheral nerve, spinal cord and brain [4, 5]. DRG neurons exposed to cisplatin underwent apoptosis likely via aberrant re-entry into the cell cycle [6, 7]. Oxidative stress might also play an important role as anti-oxidant vitamin E was able to reduce cisplatin neuropathy in animals and patients [8, 9]. Nevertheless, the exact molecular mechanisms underlying the neuronal apoptosis induced by cisplatin remain largely unknown.

Mitogen-activated protein kinases (MAPKs), a family of serine/threonine kinases, have been shown to play a role in cisplatin-induced apoptosis of tumor cells [10]. In mammalian cells, three subfamilies of MAPKs including extracellular signal regulated kinase

(ERK), c-Jun amino-terminal kinase (JNK) and p38 kinase (p38) have been identified. Signaling pathways of MAPKs transduce extracellular stimuli to altered gene expression resulting in cell proliferation, differentiation and apoptosis. In cancer cells exposed to cisplatin, ERK, JNK, and p38 had either pro-apoptotic or anti-apototic roles depending on cell type, proliferation and differentiation status [10]. Activation of p38 has been linked to nephrotoxicity, another major side effects of cisplatin [11]. More relevant to cisplatin neuropathy, ERK and p38 were activated in DRG culture and led to apoptosis while JNK had an opposite role [12]. These roles of MAPKs have not been confirmed in the animal model of cisplatin neuropathy. Therefore, the aim of this study was to examine the phosphorylation of MAPKs in the peripheral nervous system of rats treated with cisplatin.

Materials and methods

Eighty female Wistar rats weighing 200 to 250 g were housed in aluminum cages on a 12-hour light-dark cycle with access to food and water ad libitum. This experiment was approved by the Institutional Ethics Committee, Faculty of Medicine, Chulalongkorn University and was carried out in accordance with the guidelines of the National Research Council of Thailand which covers the ethical standard for animal studies. All efforts were done to minimize pain and discomfort.

Drug administration

The animals were divided into two groups: control (C) and cisplatin (P) (n = 40 each). The cisplatin group received cisplatin (Pfizer) 2 mg/kg intraperitoneally, twice a week, for five consecutive weeks (20 mg/kg accumulative dose). Cisplatin was diluted in normal saline to the final concentration of 0.5 mg/ml. The dilution was aimed to give excess fluid to prevent nephrotoxicity. Physiological and structural abnormalities of peripheral nerve were induced with this dose and schedule of cisplatin injection [13]. The control group received only normal saline. Body weight was recorded before each injection and once a week after cessation of treatment.

Hind-paw thermal threshold

The animals were allowed to familiarize themselves with the test procedure and apparatus. The test was done at baseline and the first, third, fifth, eighth, and twelfth weeks after the start of cisplatin injection. Each rat was placed on the hot plate analgesia meter (Harvard Apparatus, UK) maintained at 55°C. When the rat licked its hind paw on either side, elapsed time was recorded as a latency. The cut-off duration of 35 seconds was employed to avoid skin injury. If the latency was over this limit, 35 seconds was used for further analysis. The test was repeated at least three times with an interval of 15 minutes and an average latency was obtained for each rat.

Hind-paw mechanical threshold

Von Frey filaments with bending forces ranging from 0.1 to 40 g were used to measure the mechanical threshold at baseline and the first, third, fifth, eighth, and twelfth weeks. Each rat was placed on a plastic mesh. The plantar surface of the right hind paw was stimulated by starting with the smallest filament. Each stimulus was applied for approximately one second. If withdrawal of hind paw did not occur, the next larger filament in the series was applied in a similar manner. When the hind paw was withdrawn from a particular filament after at least four out of five applications, the force value of that filament was considered the withdrawal threshold. The average value for each rat was calculated from the thresholds of at least three repeats with an interval of 15 minutes.

Motor nerve conduction velocity

The motor nerve conduction velocity (MNCV) was measured at baseline and the third, fifth, eighth, and twelfth weeks. The rat was anesthetized using isoflurane and rectal temperature was maintained at 37±0.3°C using a heating pad and digital rectal thermometer. The stimulating and recording needle electrodes were inserted at the sciatic notch and the second interosseous muscle of the hind foot, respectively. The ground electrode was placed at the lateral side of the hind foot. These electrodes were connected to the oscilloscope (Neurostar, Oxford Instrument). The sciatic nerve was stimulated with a supramaximal stimulus and compound muscle action potential (CMAP) was recorded. Latency1 (L1) was measured from the stimulation artifact to the positive peak of M wave. The average L1 was derived from at least five stimulations. Then, the stimulating electrode was moved to the side of Achilles' tendon and the procedure was repeated to determine the average latency2 (L2). The MNCV was calculated by dividing the distance between the two stimulation points by the latency difference (L1-L2).

Tissue collection

At each time point, 12 rats (C = 6, P = 6) were sacrificed by overdose isoflurane and subsequent cardiac puncture. The sciatic nerves and L4-L6 DRG were removed immediately and snap-frozen on dry ice. These specimens were moved to -70°C and stored there until used for Western blot analysis. In addition, some L4 DRG and sciatic nerves were also used for immunohistochemistry. Sciatic nerves were fixed in 4% PFA for six hours, rinsed and stored in 30% sucrose at 4°C. DRG were fixed in 10% formalin overnight and processed for embedding in paraffin. For morphometric analysis, additional 10 rats (C = 5, P = 5) in the eighth, and twelfth weeks were transcardially perfused with 200 ml of normal saline followed by 400 ml of 4% paraformaldehyde (PFA). L4 DRG and sciatic nerves were post-fixed in 3% glutaraldehyde for six hours and embedded in epoxy resin.

Nerve morphometry

Transverse 1 μm-thick sections of the sciatic nerve were cut, mounted on slides, and stained with paraphenylenediamine. The sections were examined under a light microscope and the cross-sectional areas were chosen using the three-window sampling method. Details of this sampling technique were described elsewhere [14]. Briefly, under 40x objective lens, three windows of 0.012 mm^2 were randomly placed, one in the middle and the other two in the periphery of fascicle. Images of these windows were imported into the microcomputer via a CCD camera. Morphometric analysis was done to obtain the number of myelinated fibers, axon diameter, myelinated fiber density, myelin thickness, and g ratio using the Image-Pro Plus software. The values derived from the three windows were extrapolated to the whole nerve.

DRG morphometry

The DRG were serially cut into 2 μm-thick sections and stained with toluidine blue. The estimation for total number of neurons in each ganglion was done using the physical dissector method modified from those reported by Tredici et al [15] and Schenker et al [16]. Details of the procedures were described elsewhere [17]. In brief, every twentieth section was selected and the number of neurons with prominent nucleus and nucleolus was counted. Then, this number was extrapolated to the total number for the whole DRG. Moreover, at least 300 neurons in each DRG were randomly analyzed for areas of the cell body, nucleus and nucleolus using the Image-Pro Plus software.

Western blot analysis

Sciatic nerves and pooled L4-L6 DRG were homogenized and the concentration of protein was determined using the Bramhall assay [18]. SDS-PAGE was performed on 20 and 30 μg protein for DRG and sciatic nerve, respectively. The protein was then transferred to nitrocellulose membrane using a semi-dry electroblotter. The membranes were blocked and incubated in either primary antibodies to total (T) or phosphospecific (P) forms of MAPKs: ERK (1:500 for ERK-P and 1:5,000 for ERK-T, Santa Cruz Biotechnology), JNK (1:200 for JNK-P and 1:500 for JNK-T, Santa Cruz Biotechnology) and p38 (1:500 for p38-P and 1:1,000 for p38-T, Cell Signaling Technology) for 24 hours at 4°C. The membranes were then incubated with the biotinylated secondary antibody (1:200, Vector) for 30 minutes followed by avidin and biotinylated horseradish peroxidase (HRP) (Vectastain ABC reagent, Vector) for 30 minutes. Then, diaminobenzidine (DAB) (DAB substrate kit for peroxidase, Vector) was applied on the membranes until dark-brown color developed. The specific bands were scanned and densities were analyzed using Image-Pro Plus software. Finally, the ratio of phosphorylated to total forms was calculated to represent the phosphorylation status of MAPKs. The data were normalized such that mean control values were equal to 1.

Immunohistochemistry

DRG embedded in paraffin were cut at 4 μm thickness. After deparaffinization, antigen retrieval was achieved using the pressure cooker. Then, sections were blocked and incubated with antibodies to ERK-P (1:50, Santa Cruz Biotechnology), JNK-P (1:100, Santa Cruz Biotechnology) and p38-P (1:100, Cell Signaling Technology) for 24 hours at 4°C. On the next day, the sections were incubated with the biotinylated secondary antibody (1:200, Vector) for 40 minutes, followed by fluorescein avidin (1:200, Vector) for 30 minutes. After mounting, the slides were examined under a fluorescence microscope. The nerves stored in 30% sucrose were embedded in OCT medium and longitudinally cut at 10-□m thickness using a cryostat. The sections were processed in the same way as described above except the application of

double staining using anti-S-100 antibody (1:100, Chemicon) followed by rhodamine avidin (1:200, Vector) to identify Schwann cells.

Statistical analysis

Student's t-test was used to compare mean body weight, thermal latencies, mechanical latencies, MNCV, morphometric parameters, and phosphorylation ratio of MAPKs between the control and cisplatin groups at each time point. This test was done using SPSS for Windows version 10. Statistically significant differences were considered when $p < 0.05$.

Results

Control rats showed continuous weight gain over the study period as shown in **Figure 1**. In contrast, body weight of the cisplatin group started to decrease significantly compared with that of the control group in the third week and remained lower until the end of study.

Hind-paw thermal threshold

Heat latency of the cisplatin group was significantly prolonged relative to that of the control group in the fifth week (**Figure 2**), indicating transient thermal hypoalgesia. The latencies were similar between the two groups thereafter.

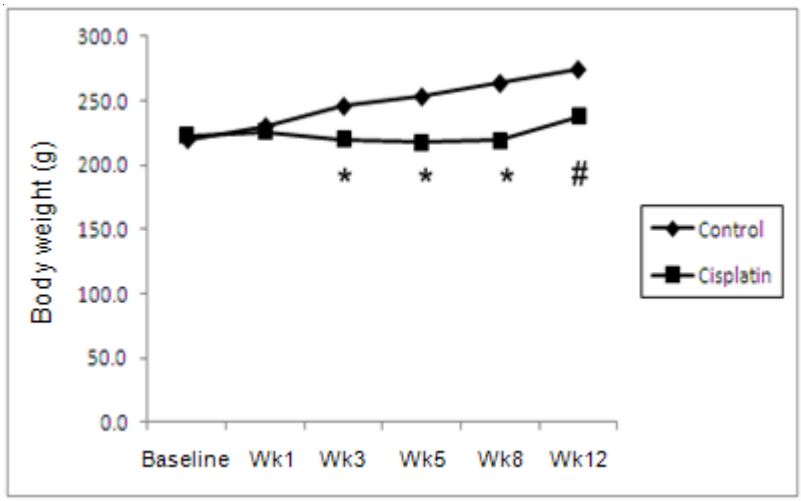

Figure 1. Changes in the average body weight of the control (C) and cisplatin (P) groups. *p <0.001 between C and P, #p <0.01 between C and P

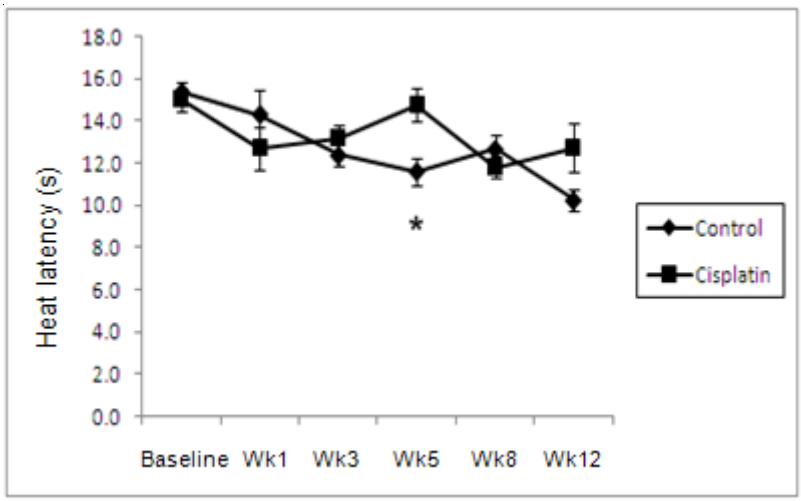

Figure 2. Changes in the heat latency of the control (C) and cisplatin (P) groups. Data are means±SEM. *p <0.01 between C and P

Hind-paw mechanical threshold

Only trends toward decrease in mechanical threshold were found in the cisplatin compared with the control groups in the third and fifth weeks (**Figure 3**). This reduction was fully recovered thereafter.

Control rats had increasing sciatic MNCV from baseline to the twelfth week (**Figure 4**). However, the MNCV of the cisplatin-treated rats remained constant from the third and twelfth weeks. Therefore, the significantly lower MNCV was observed in the cisplatin-treated rats from the fifth week until the end of study.

Nerve morphometry

Myelin thickness of the cisplatin group was significantly decreased relative to that of the control group in the eighth and twelfth weeks (**Table 1**). As for the diameter of myelinated axons, the value of the cisplatin group was significantly higher than that of the control group in the eighth week but became lower in the twelfth week. The increase in the axon diameter of the cisplatin group resulted in higher g ratio. Reduced number of myelinated fibers observed in the cistplatin-treated rats compared with the controls at both time points was not statistically significant. Similarly, no significant changes in the myelinated fiber density were detected.

DRG morphometry

Cisplatin-treated rats had significantly decreased somatic, nuclear and nucleolar areas of L4 DRG neurons compared with the controls in the eighth and twelfth weeks (**Table 2**). The number of neurons tended to decrease in the cisplatin group at both time points.

Phosphorylation of MAPKs in the DRG

Phosphorylation ratio of ERK in the DRG was not consistent over the study period. The most striking change was the increased phosphorylation in the twelfth week (**Figure 5**). However, this change was not statistically significant. It is worth noting that expression of ERK-T was unchanged throughout the study period (data not shown). As for JNK, phosphorylation was significantly higher in the cisplatin-treated compared to control rats in the first week and returned to the levels similar to those of controls thereafter (**Figure 6**). Expression of JNK-T was comparable between the two groups at all time points (data not shown). p38 phosphorylation was significantly decreased in the cisplatin relative to control groups in the first week (**Figure 7**). The phosphorylation in the cisplatin group was then gradually increased until reaching the control levels at later time points. Levels of p38-T were similar between the two groups throughout the study period.

Immunohistochemistry results showed that ERK-P was localized in the nuclei and satellite cells of large DRG neurons from the control and cisplatin-treated rats (**Figure 8A** and **B**). Moreover, ERK-P was also found in the cytoplasm of small- to medium-sized neurons. In contrast, JNK-P was prominently found in neuronal nuclei in both groups (**Figure 8C** and **D**). As for p38-P, its immunoreactivity was mainly observed in the neuronal nuclei and cytoplasm of small- to medium-sized neurons (**Figure 8E** and **F**). No differences in the location of these MAPKs were observed between groups and among different time points.

Phosphorylation of MAPKs in the sciatic nerve

ERK phosphorylation was significantly higher in the cisplatin compared with the control groups in the eighth week, but not other time points (**Figure 9**). Phosphorylation of JNK was significantly elevated in the cisplatin-treated relative to the control rats in the first week (**Figure 10**). However, the levels of JNK-P at later time points were too low to be quantitatively analyzed. p38 phosphorylation was not significantly different between the two groups in the first week. Similar to JNK-P, p38-P was hardly detected at later time points. Levels of total MAPKs were comparable between groups at all time points.

JNK-P was predominantly localized in the Schwann cells indicated by co-localization with S-100 (**Figure 11C** and **D**). In contrast, p38-P was mainly observed in the axons as it was not co-localized with S-100 (**Figure 11E** and **F**). ERK-P immunoreactivitiy was seen in both axons and Schwann cells (**Figure 11A** and **B**). These patterns of MAPK immunoreactivities were not different between groups and among various time points.

The significant changes in the functional and pathological aspects including MAPK phosphorylation are summarized in **Table 3**.

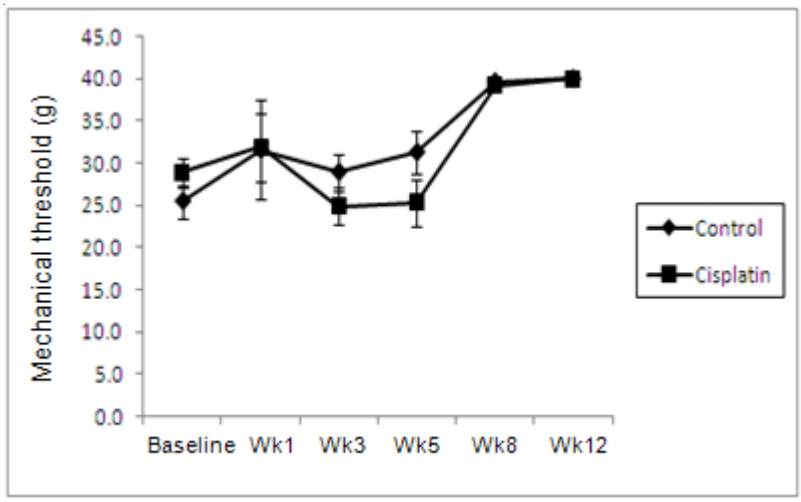

Figure 3. Changes in the mechanical threshold of the control and cisplatin groups. Data are means±SEM.

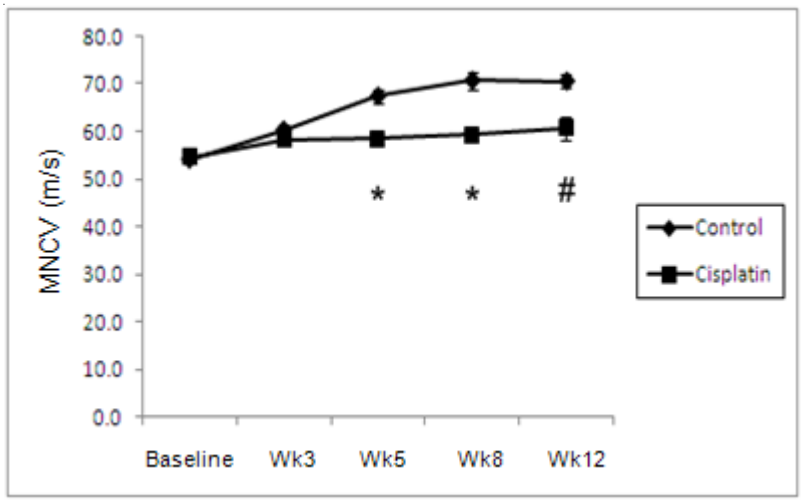

Figure 4. Changes in the sciatic motor nerve conduction velocity (MNCV) of the control (C) and cisplatin (P) groups. Data are means±SEM. *p <0.001 between C and P, #p <0.01 between C and P

Table 1. Morphometric data of sciatic nerve

Group	Axon diameter (μm)	Myelin thickness (μm)	g ratio	Fiber density (/mm^2)	No. of fiber
Week 8					
Control (C)	3.41±0.11	1.35±0.02	0.56±0.01	17,131.9±726.3	8,654±288
Cisplatin (P)	3.89±0.04*	1.27±0.02*	0.60±0.01#	15,500.0±295.9	7,958±103
Week 12					
Control (C)	3.90±0.07	1.42±0.04	0.58±0.01	15,188.9±618.2	8,277±279
Cisplatin (P)	3.76±0.04*	1.31±0.02*	0.58±0.01	16,466.7±1,012.7	8,092±255

Data are means±SEM, *p <0.05, #p< 0.01 vs. C at the same time point

Table 2. Morphometric data of L4 DRG

Group	Somatic area (μm²)	Nuclear area (μm²)	Nucleolar area (μm²)	No. of neuron
Week 8				
Control (C)	1,035.0±29.9	162.3±1.4	12.6±0.1	20,265±1,598
Cisplatin (P)	911.0±32.4*	148.3±5.3*	10.5±0.4#	16,530±1,696
Week12				
Control (C)	1,115.8±31.6	161.1±3.0	14.9±0.2	19,785±1,871
Cisplatin (P)	842.6±39.2#	133.8±5.1#	10.9±0.9#	16,346±1,643

Data are means±SEM, *p <0.05, #p < 0.01 vs. C at the same time point

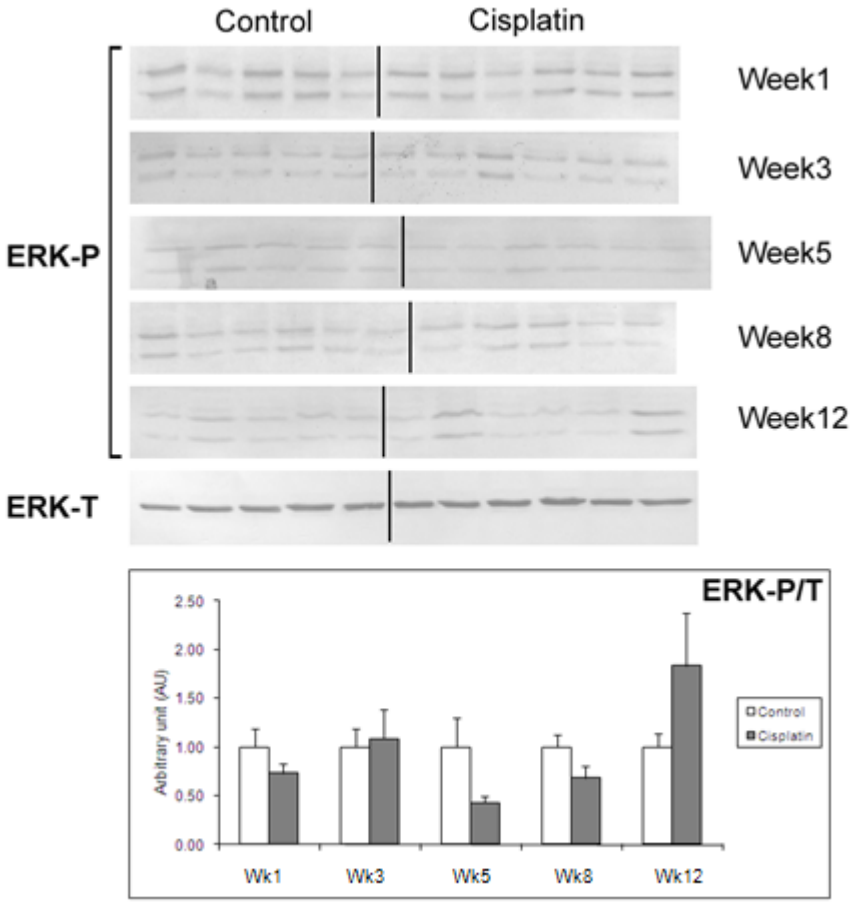

Figure 5. ERK phosphorylation in L4-6 DRG from the control and cisplatin groups. Immunoblots probed for ERK-P at various time points are shown above. Since the levels of ERK-T were not different between groups at any time point, the representative blot is shown here. For ERK-P, two isoforms were observed (ERK1 at 44 kDa and ERK2 at 42 kDa), whereas they were not distinguishable in ERK-T. The bar chart demonstrates the ratio of ERK-P to ERK-T. Data are means±SEM.

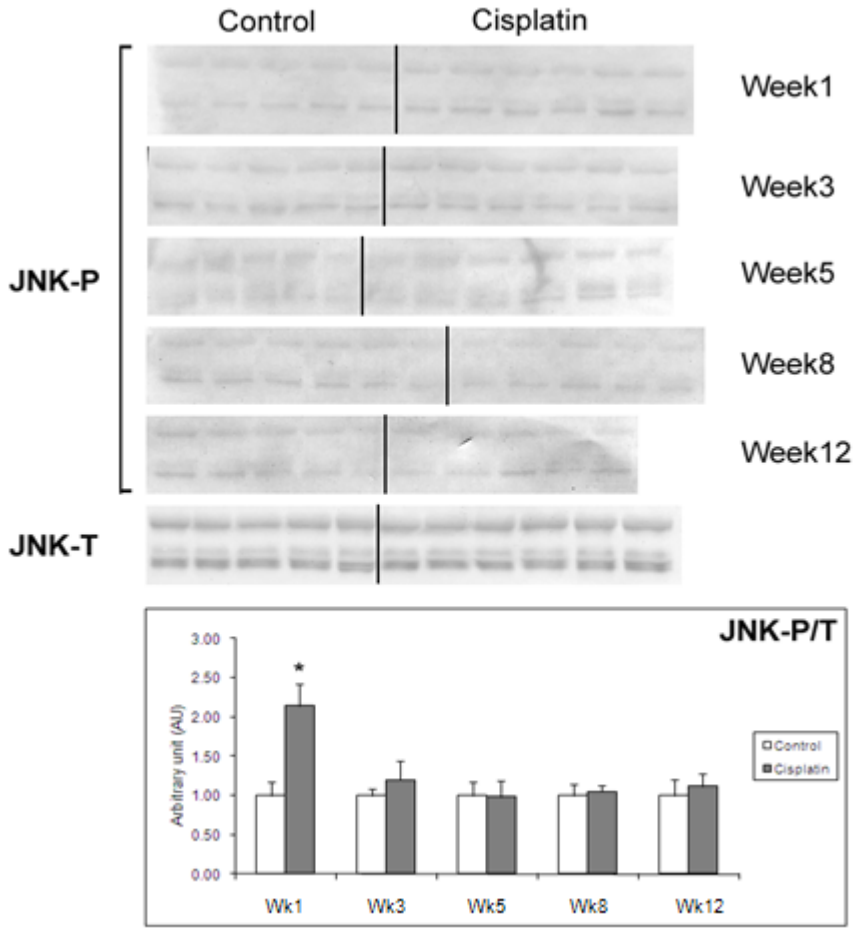

Figure 6. JNK phosphorylation in L4-6 DRG from the control and cisplatin groups. Immunoblots probed for JNK-P at various time points are shown above. Since the levels of JNK-T were not different between groups at any time point, the representative blot is shown here. Three isoforms of JNK were observed at 56, 54, and 46 kDa. The bar chart demonstrates the ratio of JNK-P to JNK-T. Data are means±SEM. *p <0.01 vs. control

Discussion

Behavioral, electrophysiological, and morphological assessments were done to confirm if cisplatin-treated rats developed peripheral neuropathy and to examine temporal changes in these parameters. An accumulative dose of cisplatin 20 mg/kg over five weeks induced significant weight loss, which persisted after the last injection. This was consistent with other studies using similar dose regimens [13, 19-21]. Transient thermal hypoalgesia in the fifth week and slightly decreased mechanical threshold in the third and fifth weeks were also observed. Thermal hypoalgesia and mechanical allodynia after cisplatin treatment were previously reported [13, 19-22]. The MNCV was significantly slower in the cisplatin group from the fifth until the twelfth weeks. Two previous studies have reported no involvement of the MNCV after cisplatin treatment [23, 24]. This discrepancy might be due to different doses of cisplatin used, as ours were much higher. This view was also supported by Virdu et al, which found reduced MNCV only after high accumulative doses [25].

Morphometric analysis of DRG from the cisplatin-treated rats revealed significant atrophies of neuronal soma, nucleus, and nucleolus. These changes were evident late in the course of cisplatin treatment and persisted several weeks after the last injection. This was supported by similar findings in previous studies [19, 21, 26-28]. Sciatic nerves from the cisplatin group showed significant thinning of the myelin sheath in the eighth and twelfth weeks. The axon diameter was significantly increased in the eighth week but decreased in the twelfth week. There were no significant changes in the number and density of

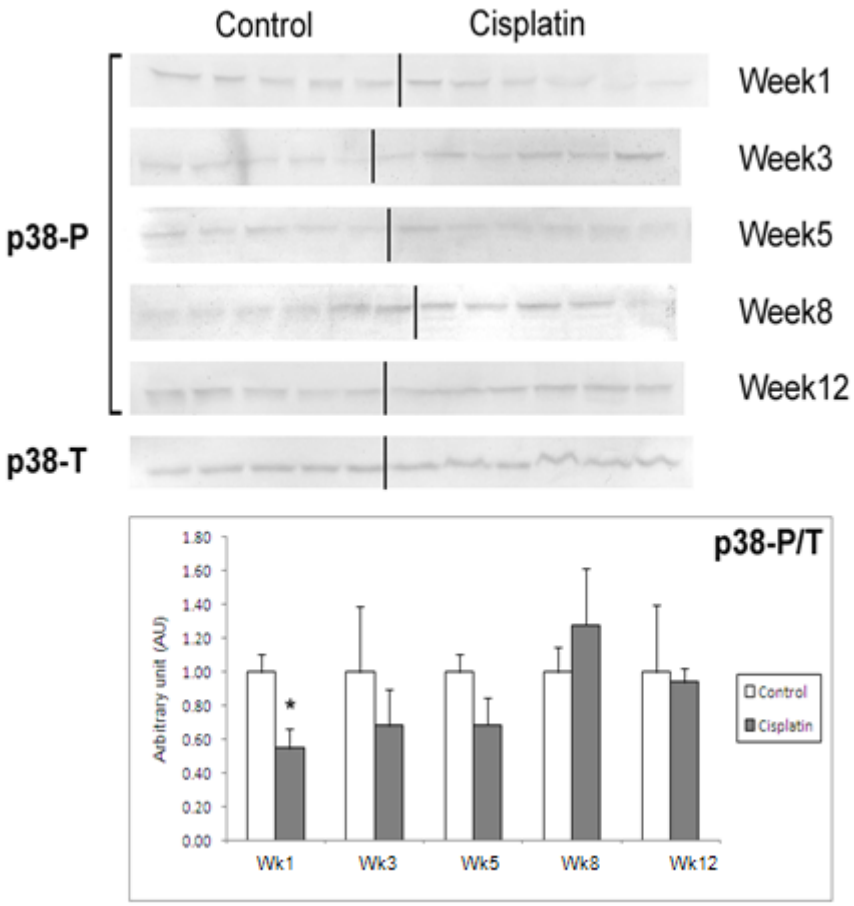

Figure 7. p38 phosphorylation in L4-6 DRG from the control and cisplatin groups. Immunoblots probed for p38-P at various time points are shown above. Since the levels of p38-T were not different between groups at any time point, the representative blot is shown here. The bar chart demonstrates the ratio of p38-P to p38-T. Data are means±SEM. *p <0.05 vs. control

myelinated fibers between groups at both time points. Significant decrease in the myelinated fiber diameter with mildly reduced number of fibers induced by cisplatin was also found by other studies [15, 27, 28]. No morphometric evaluation of myelin thickness has been previously done but observation in two studies did not detect myelin abnormalities [13, 27]. Reduced myelin thickness in this study could explain the slowing of MNCV observed in the same period. Underlying mechanisms of this abnormality are still unclear but apoptosis of Schwann cells induced by cisplatin [29] might be responsible. According to the transient increase in the axon diameter, axonal swelling might be the cause. This condition was conflicting with axonal atrophy observed in previous studies [15, 27, 28]. The inconsistency might be due to different time points used (several weeks after the last cisplatin injection in this study vs. just after the last dose in other studies). Since the mechanisms responsible for cisplatin-induced axonopathy remain unclear, those underlying the axonal swelling are unknown. Nevertheless, the axonal swelling was also observed in vincristine neuropathy [30] and occasionally in neuropathies caused by acrylamide [31] and γ-diketone [32]. Thus, the axon swelling seen in this study was likely real and required further investigations.

Regarding the functional and pathological abnormalities described above, we have proved that the dose regimen of cisplatin used in this study could induce peripheral neuropathy. The next step was to examine temporal changes in the MAPK phosphorylation. We found that cisplatin significantly enhanced the ERK phosphorylation in the sciatic nerve in the eighth week but insignificantly in the DRG in the twelfth week. These data suggested that ERK was activated by cisplatin more intensely and early

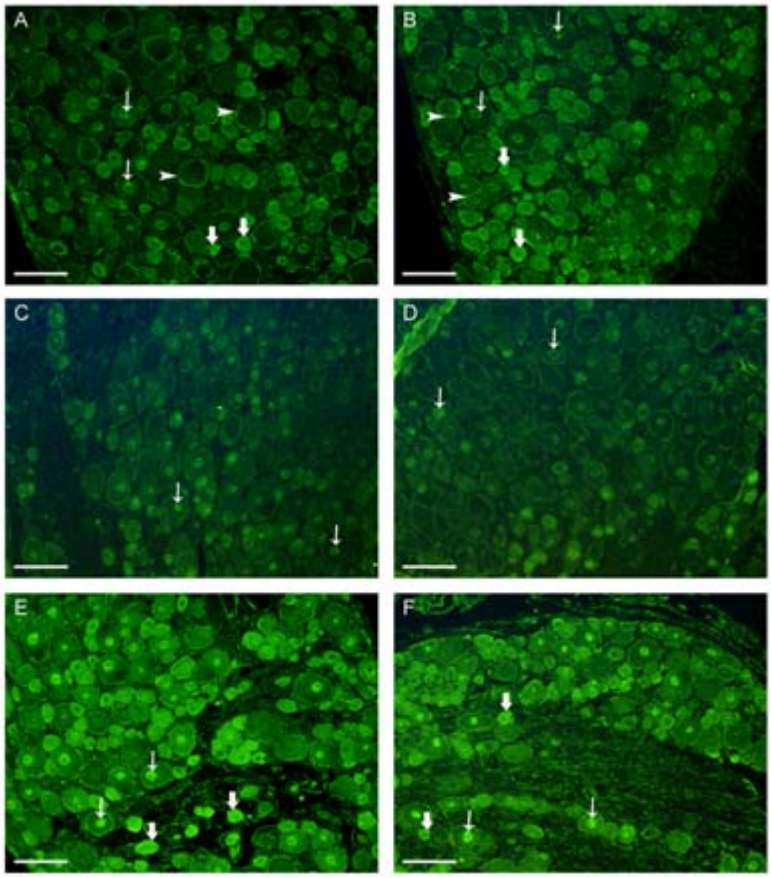

Figure 8. Immunoreactivity of phosphorylated MAPKs in the L4 DRG from the control (**A, C, E**) and cisplatin (**B, D, F**) groups. ERK-P (**A, B**), JNK-P (**C, D**), p38-P (**E, F**). Thin and thick arrows indicate positive immunoreactivity in neuronal nuclei and cytoplasm of small- to medium-sized neurons, respectively. Arrowheads indicate positive immunoreactivity in satellite cells around cell bodies of large neurons. Scale bars represent 100 μm.

in the sciatic nerve than the DRG. As for JNK, its phosphorylation in both sciatic nerve and DRG was significantly higher in the cisplatin group only at the first week. In contrast, phosphorylation of p38 was significantly inhibited in the DRG, but not in the sciatic nerve, from the cisplatin-treated rats in the first week. Immunohistochemistry revealed that active MAPKs were mainly found in DRG neurons. However, ERK-P was additionally seen in the satellite cells. These findings were similar to what has been reported [33]. In the sciatic nerve, JNK-P was found mainly in the Schwann cells while p38-P was localized to the axons. ERK-P was seen in both structures. No changes in the locations of these MAPKs between the control and cisplatin groups indicated that further activation of MAPKs in the same compartments was responsible for increased phosphorylation in the cisplatin group seen in Western blot results.

In an attempt to further elucidate the role of these activated MAPKs in cisplatin neuropathy, we compared the temporal aspects of functional disorders and MAPK phosphorylation. Since functional impairments were observed as early as the third week, these abnormalities were unlikely related to the altered MAPK phosphorylation. In contrast, the morphological abnormalities appeared later from the eighth week onward which was the same period of ERK activation. Therefore, since its persistent activation was correlated with the appearance of pathological abnormalities, ERK could be the potential pathway responsible for this parameter of cisplatin-induced neuropathy. On the other hand, this may only represent another event in parallel.

Existing evidence can shed some light on the possible role of MAPKs in cisplatin neuropathy. In vitro, all three MAPKs have been linked to

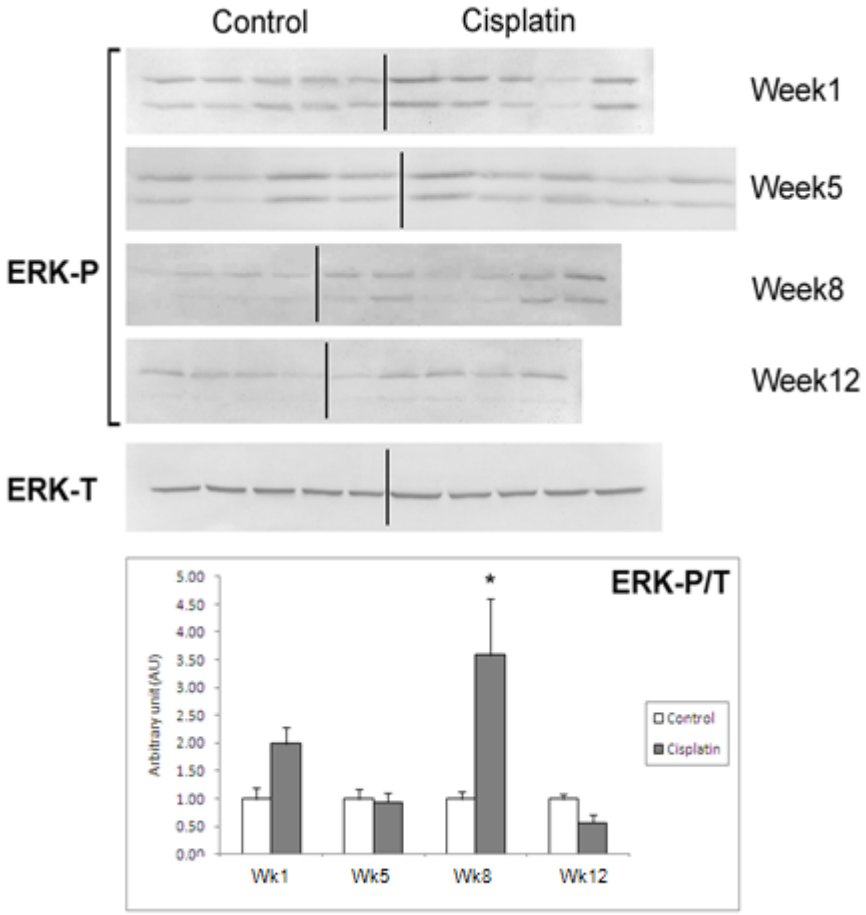

Figure 9. ERK phosphorylation in the sciatic nerve from the control and cisplatin groups. Immunoblots probed for ERK-P at various time points are shown above. Since the levels of ERK-T were not different between groups at any time point, the representative blot is shown here. The bar chart demonstrates the ratio of ERK-P to ERK-T. Data are means±SEM. **p* <0.05 vs. control

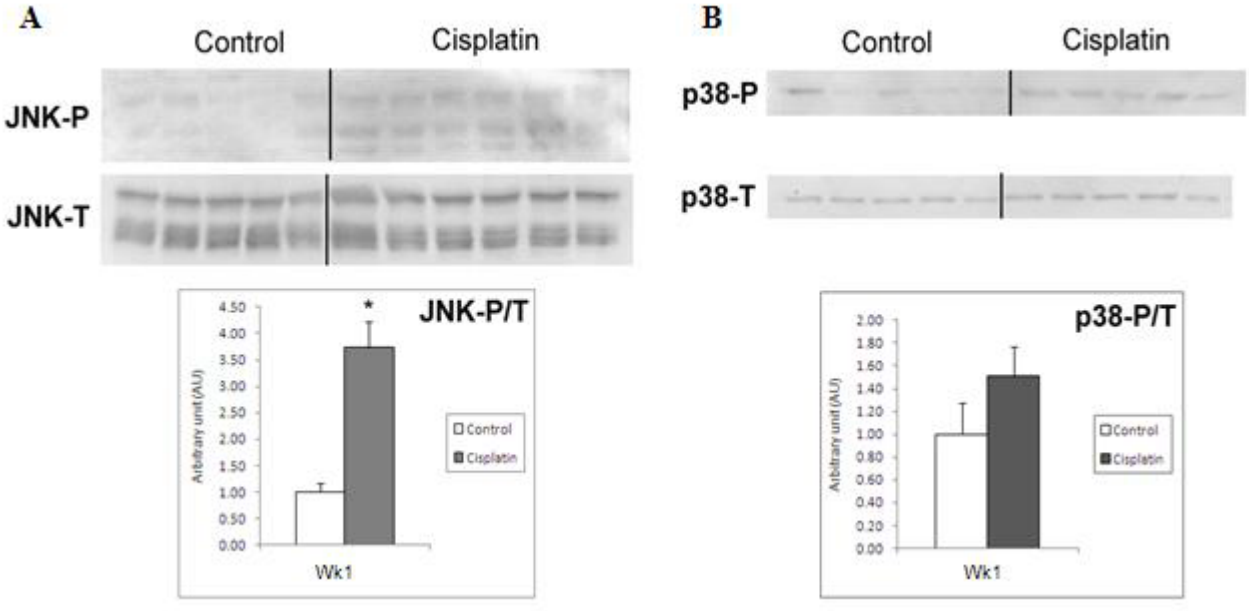

Figure 10. Phosphorylation of JNK (**A**) and p38 (**B**) in the sciatic nerve from the control and cisplatin groups in the first week. Immunoblots probed for JNK-P, JNK-T, p38-P, and p38-T are shown above. The bar charts demonstrate the ratio of JNK-P to JNK-T and p38-P to p38-T. Data are means±SEM. **p* <0.05 vs. control

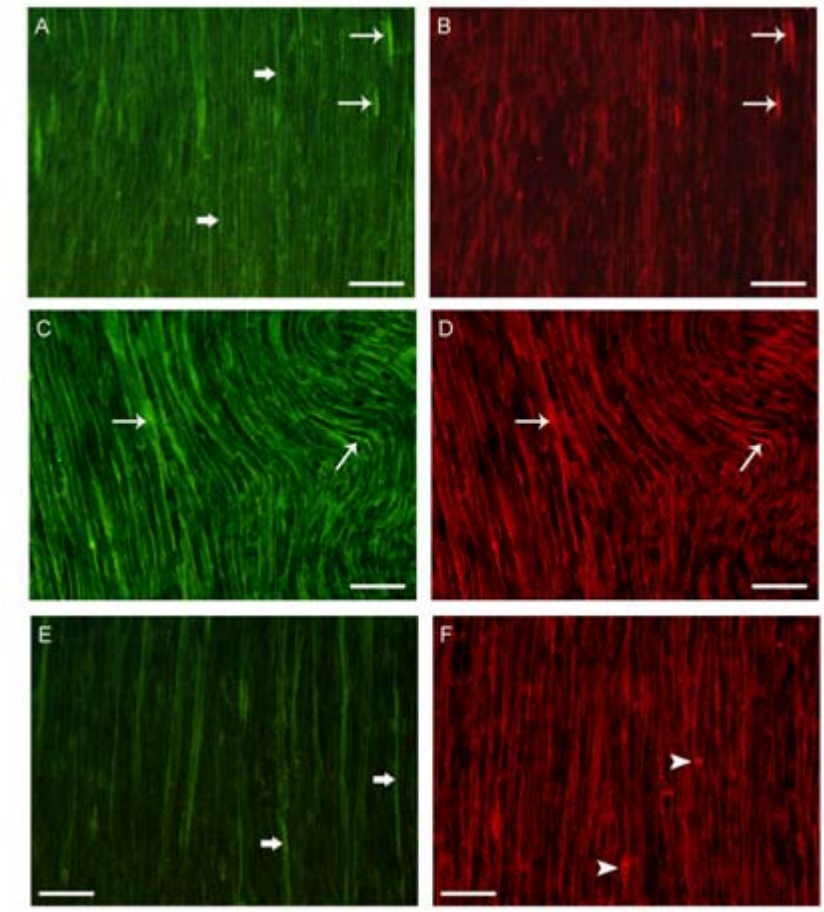

Figure 11. Immunoreactivity of phosphorylated MAPKs (MAPK-P) in the longitudinal sections of sciatic nerve. The sections were double stained for MAPK-P (green - left column) and S-100 (red - right column) with the same areas in both columns. ERK-P (**A**), JNK-P (**C**), p38-P (**E**). Since there were no differences in the results between groups and among time points, representative images are shown here. Thick and thin arrows indicate MAPK-P immunoreactivity in the axons (not co-localized with S-100) and Schwann cells (co-localized with S-100), respectively. Arrowheads indicate S-100 immunoreactivity in the Schwann cells. Scale bars represent 50 μm.

Table 3. Summary of important results

Parameter	Week 1	Week 3	Week 5	Week 8	Week 12
Thermal threshold	↔	↔	↑	↔	↔
Mechanical threshold	↔	↓	↓	↔	↔
Sciatic MNCV	↔	↔	↓	↓	↓
Abnormal morphometry	-	-	-	√	√
ERK-P in DRG	↔	↔	↔	↔	↑
ERK-P in sciatic nerve	↔	↔	↔	↑	↔
JNK-P in DRG	↑	↔	↔	↔	↔
JNK-P in sciatic nerve	↑	-	-	-	-
p38-P in DRG	↓	↔	↔	↔	↔
p38-P in sciatic nerve	↔	-	-	-	-

↔ not different between the control and cisplatin groups
↑/↓ significantly increased/decreased in the cisplatin vs. control groups
/ trend toward increase/decrease in the cisplatin vs. control groups
- not determined

neuronal apoptosis in response to various stresses [34-37]. Moreover, emerging roles of MAPKs in peripheral neuropathies, especially diabetic and chemotherapeutic-induced neuropathies, were also evident [38]. Activation of ERK with neuroprotective effect was also shown in primary cortical neurons exposed to cisplatin [39]. In the more closely related model, Scuteri and co-workers have studied the role of MAPKs in primary DRG culture treated with cisplatin [12]. They found that cisplatin induced early and sustained p38 activation leading to apoptosis. In contrast, JNK was temporarily activated later and had a neuroprotective role. ERK had the pro-apoptotic role but its activation was late and less dramatic. Comparing with our results, the consistent data included the late and small activation of ERK in the DRG (twelfth week in this study). Activation of JNK and inhibition of p38 were temporary and early which was different from Scuteri et al. The conflicting results might be due to different models used (in vitro vs. in vivo). In addition, we have also examined the phosphorylation of MAPKs in the sciatic nerve and found that ERK was highly activated in the eighth week while JNK was activated in the first week. According to the immunohistochemistry results, ERK-P was observed in both axons and Schwann cells while JNK-P was found mainly in the latter. Therefore, it is possible that ERK was activated in Schwann cells and axons simultaneously. Then, ERK-P was retrogradely transported along the axons and resulted in the increased level of ERK-P in the cell bodies of DRG neurons. The axonal transport of ERK has been previously demonstrated [40]. As for JNK, due to the very low level of JNK-P in the axons and the same activation time in the DRG and sciatic nerve, activated JNK in the DRG neurons and Schwann cells was probably separate. In addition, due to its very early and transient nature, this JNK activation might be only the acute reaction to stresses and its significance was likely minimal. In case of p38, the role of its temporary activation in only DRG in the first week was unknown and its implication was probably trivial. This was in contrast with the cisplatin-induced persistent activation of p38 leading to apoptosis in the DRG culture [15].

In conclusion, this study has shown that cisplatin activated ERK first in the sciatic nerve and later in the DRG. The time points of activation were correlated with those of morphological changes. In contrast, the activation of JNK in both DRG and sciatic nerve with inhibition of p38 in the DRG occurred transiently prior to the pathological changes. Hence, the ERK pathway might play a role in structural alterations in cisplatin-induced neuropathy. This hypothesis must be proved by future studies using the ERK inhibitor.

Acknowledgement

This work was supported by Rachadaphisek-somphot Fund 2008 from the Faculty of Medicine, Chulalongkorn University (SA) and the 90th anniversary of Chulalongkorn University Fund 3/2009 (Ratchadaphiseksomphot Endowment Fund) (TW, VC). All authors have made significant contributions to the work. The authors have no conflict of interest to report.

References

1. Boulikas T, Vougiouka M. Recent clinical trials using cisplatin, carboplatin and their combination chemotherapy drugs (review). Oncol Rep. 2004; 11: 559-95.
2. Krarup-Hansen A, Fugleholm K, Helweg-Larsen S, Hauge EN, Schmalbruch H, Trojaborg W, et al. Examination of distal involvement in cisplatin induced neuropathy in man. An electrophysiological and histological study with particular reference to touch receptor function. Brain. 1993; 116:1017-41.
3. Krarup-Hansen A, Helweg-Larsen S, Schmalbruch H, Rorth M, Krarup C. Neuronal involvement in cisplatin neuropathy: prospective clinical and neurophysiological studies. Brain. 2007; 130:1076-88.
4. McDonald ES, Randon KR, Knight A, Windebank AJ. Cisplatin preferentially binds to DNA in dorsal root ganglion neurons in vitro and in vivo: a potential mechanism for neurotoxicity. Neurobiol Dis. 2005; 18:305-13.
5. Dzagnidze A, Katsarava Z, Makhalova J, Liedert B, Yoon MS, Kaube H, et al. Repair capacity for platinum-DNA adducts determines the severity of cisplatin-induced peripheral neuropathy. J Neurosci. 2007; 27: 9451-7.
6. Gill JS, Windebank AJ. Cisplatin-induced apoptosis in rat dorsal root ganglion neurons is associated with attempted entry into the cell cycle. J Clin Invest. 1998; 101:2842-50.
7. Fischer SJ, McDonald ES, Gross L, Windebank AJ. Alterations in cell cycle regulation underlie cisplatin induced apoptosis of dorsal root ganglion neurons in vivo. Neurobiol Dis. 2001; 8:1027-35.
8. Leonetti C, Biroccio A, Gabellini C, Scarsella M, Maresca V, Flori E, et al. α-tocopherol protects againt

cisplatin-induced toxicity without interfering with antitumor efficacy. Int J Cancer. 2003; 104:243-50.
9. Pace A, Giannarelli D, Gali□ E, Savarese A, Carpano S, Della Giulia M, et al. Vitamin E neuroprotection for cisplatin neuropathy a randomized, placebo-controlled trial. J Neurology. 2010; 74:762-6.
10. Brozovic A, Osmak M. Activation of mitogen-activated protein kinases by cisplatin and their role in cisplatin-resistance. Cancer Lett. 2007; 251:1-16.
11. Ramesh G, Reeves WB. p38 MAP kinase inhibition ameliorates cisplatin nephrotoxicity in mice. Am J Physiol Renal Physiol. 2005; 289:F166-74.
12. Scuteri A, Galimberti A, Maggioni D, Ravasi M, Pasini S, Nicolini G, et al. Role of MAPKs in platinum-induced neuronal apoptosis. Neurotoxicology. 2009; 30:312-9.
13. Authier N, Gillet JP, Fialip J, Eschalier A, Coudore F. An animal model of nociceptive peripheral neuropathy following repeated cisplatin injections. Exp Neurol. 2003; 182:12-20.
14. Chentanez V, Cha-oumphol P, Kaewsema A, Agthong S, Huanmanop T. Accuracy of the three-window sampling method in morphometric analysis of human sural nerve. J Neurosci Methods. 2006; 157:154-7.
15. Tredici G, Braga M, Nicolini G, Miloso M, Marmiroli P, Schenone A, et al. Effect of recombinant human nerve growth factor on cisplatin neurotoxicity in rats. Exp Neurol. 1999; 159:551-8.
16. Schenker M, Kraftsik R, Glauser L, Kuntzer T, Bogousslavsky J, Barakat-Walter I. Thyroid hormone reduces the loss of axotomized sensory neurons in dorsal root ganglia after sciatic nerve transection in adult rat. ExpNeurol. 2003; 184:225-36.
17. Wongtawatchai T, Agthong S, Kaewsema A, Chentanez V. Sex-related differences in cisplatin-induced neuropathy in rats. J Med Assoc Thai. 2009; 92:1485-91.
18. Bramhall S, Noack N, Wu M, Loewenberg JR. A simple colorimetric method for determination of protein. Anal Biochem. 1969; 31:146-8.
19. Tredici G, Tredici S, Fabbrica D, Minoia C, Cavaletti G. Experimental cisplatin neuronopathy in rats and the effect of retinoic acid administration. J Neurooncol. 1998; 36:31-40.
20. Boyle FM, Wheeler HR, Shenfield GM. Amelioration of experimental cisplatin and paclitaxel neuropathy with glutamate. J Neurooncol. 1999; 41:107-16.
21. Ozturk G, Erdogan E, Anlar O, Kosem M, Taspinar M. Effect of leukemia inhibitory factor in experimental cisplatin neuropathy in mice. Cytokine. 2005; 29: 31-41.
22. Hori K, Ozaki N, Suzuki S, Sugiura Y. Upregulations of P2X(3) and ASIC3 involve in hyperalgesia induced by cisplatin administration in rats. Pain. 2010; 149:393-405.
23. Muller LJ, Gerritsen vdH, Moorer-van Delft CM, Gispen WH, Roubos EW. Morphological and electrophysiological study of the effects of cisplatin and ORG.2766 on rat spinal ganglion neurons. Cancer Res. 1990; 50:2437-42.
24. Bardos G, Moricz K, Jaszlits L, Rabloczky G, Tory K, Racz I, et al. BGP-15, a hydroximic acid derivative, protects against cisplatin- or taxol induced peripheral neuropathy in rats. Toxicol Appl Pharmacol. 2003; 190: 9-16.
25. Verd□ E, Vilches JJ, Rodr□guez FJ, Ceballos D, Valero A, Navarro X. Physiological and immunohistochemical characterization of cisplatin-induced neuropathy in mice. Muscle Nerve. 1999; 22:329-40.
26. Schmidt Y, Unger JW, Bartke I, Reiter R. Effect of nerve growth factor on peptide neurons in dorsal root ganglia after taxol or cisplatin treatment and in diabetic (db/db) mice. Exp Neurol. 1995; 132:16-23.
27. Cavaletti G, Tredici G, Marmiroli P, Petruccioli MG, Barajon I, Fabbrica D. Morphometric study of the sensory neuron and peripheral nerve changes induced by chronic cisplatin (DDP) administration in rats. Acta Neuropathol. 1992; 84:364-71.
28. Barajon I, Bersani M, Quartu M, Del Fiacco M, Cavaletti G, Holst JJ, et al. Neuropeptides and morphological changes in cisplatin-induced dorsal root ganglion neuronopathy. Exp Neurol. 1996; 138:93-104.
29. Jirsova K, Mandys V, Gispen WH, Bar PR. Cisplatin-induced apoptosis in cultures of human Schwann cells. Neurosci Lett. 2006; 392:22-6.
30. Tanner KD, Levine JD, Topp KS. Microtubule disorientation and axonal swelling in unmyelinated sensory axons during vincristine-induced painful neuropathy in rat. J Comp Neurol. 1998; 395:481-92.
31. Lehning EJ, Persaud A, Dyer KR, Jortner BS, LoPachin RM. Biochemical and morphologic characterization of acrylamide peripheral neuropathy. Toxicol Appl Pharmacol. 1998; 151:211-21.
32. Lehning EJ, Jortner BS, Fox JH, Arezzo JC, Kitano T, LoPachin RM. gamma-diketone peripheral neuropathy. I. Quality morphometric analyses of axonal atrophy and swelling. Toxicol Appl Pharmacol. 2000; 165: 127-40.
33. Obata K, Yamanaka H, Kobayashi K, Dai Y, Mizushima T, Katsura H, et al. Role of mitogen-activated protein kinase activation in injured and intact primary afferent neurons for mechanical and heat hypersensitivity after

spinal nerve ligation. J Neurosci. 2004; 24:10211-22.
34. Kawasaki H, Morooka T, Shimohama S, Kimura J, Hirano T, Gotoh Y, et al. Activation and involvement of p38 mitogen-activated protein kinase in glutamate-induced apoptosis in rat cerebellar granule cells. J Biol Chem. 1997; 272:18518-21.
35. Satoh T, Nakatsuka D, Watanabe Y, Nagata I, Kikuchi H, Namura S. Neuroprotection by MAPK/ERK kinase inhibition with U0126 against oxidative stress in a mouse neuronal cell line and rat primary cultured cortical neurons. Neurosci Lett. 2000; 288:163-6.
36. Harding TC, Xue L, Bienemann A, Haywood D, Dickens M, Tolkovsky AM, et al. Inhibition of JNK by overexpression of the JNL binding domain of JIP-1 prevents apoptosis in sympathetic neurons. J Biol Chem. 2001; 276:4531-4.
37. Junn E, Mouradian MM. Apoptotic signaling in dopamine-induced cell death: the role of oxidative stress, p38 mitogen-activated protein kinase, cytochrome c and caspases. J Neurochem. 2001; 78: 374-83.
38. Cavaletti G, Miloso M, Nicolini G, Scuteri A, Tredici G. Emerging role of mitogen-activated protein kinases in peripheral neuropathies. J Peripher Nerv Syst. 2007; 12:175-94.
39. Gozdz A, Habas A, Jaworski J, Zielinska M, Albrecht J, Chlystun M, et al. Role of N-methyl-D-aspartate receptors in the neuroprotective activation of extracellular signal-regulated kinase 1/2 by cisplatin. J Biol Chem. 2003; 278:43663-71.
40. Averill S, Delcroix JD, Michael GJ, Tomlinson DR, Fernyhough P, Priestley JV. Nerve growth factor modulates the activation status and fast axonal transport of ERK 1/2 in adult nociceptive neurones. Mol Cell Neurosci. 2001; 18:183-96.